



Integrating deep Earth dynamics in paleogeographic reconstructions of Australia

Christian Heine ^{a,*}, R. Dietmar Müller ^a, Bernhard Steinberger ^{b,1}, Lydia DiCaprio ^a

^a EarthByte Group, School of Geosciences, The University of Sydney, NSW 2006, Australia

^b Center for Geodynamics, Norges Geologiske Undersøkelse (NGU), Trondheim, Norway

ARTICLE INFO

Article history:

Received 17 February 2009

Received in revised form 14 August 2009

Accepted 31 August 2009

Available online 10 September 2009

Keywords:

Australia

Dynamic topography

Paleo-DEMs

Inundation patterns

Plate motions

Cenozoic

ABSTRACT

It is well documented that the Cenozoic progressive flooding of Australia, contemporaneous with a eustatic sea level fall, requires a downward tilting of the Australian Plate towards the SE Asian subduction system. Previously, this large-scale, mantle-convection driven dynamic topography effect has been approximated by computing the time-dependent vertical shifts and tilts of a plane, but the observed subsidence and uplift anomalies indicate a more complex interplay between time-dependent mantle convection and plate motion. We combine plate kinematics with a global mantle backward-advection model based on shear-wave mantle tomography, paleogeographic data, eustatic sea level estimates and basin stratigraphy to reconstruct the Australian flooding history for the last 70 Myrs on a continental scale. We compute time-dependent dynamic surface topography and continental inundation of a digital elevation model adjusted for sediment accumulation. Our model reveals two evolving dynamic topography lows, over which the Australian plate has progressively moved. We interpret the southern low to be caused by sinking slab material with an origin along the eastern Gondwana subduction zone in the Cretaceous, whereas the northern low, which first straddles northern Australia in the Oligocene, is mainly attributable to material subducted north and northeast of Australia. Our model accounts for the Paleogene exposure of the Gulf of Carpentaria region at a time when sea level was much higher than today, and explains anomalous Late Tertiary subsidence on Australia's northern, western and southern margins. The resolution of our model, which excludes short-wavelength mantle density anomalies and is restricted to depths larger than 220 km, is not sufficient to model the two well recorded episodes of major transgressions in South Australia in the Eocene and Miocene. However, the overall, long-wavelength spatio-temporal pattern of Australia's inundation record is well captured by combining our modelled dynamic topography with a recent eustatic sea level curve. We suggest that the apparent Late Cenozoic northward tilting of Australia was a stepwise function of South Australia first moving away northwards from the Gondwana subduction-related dynamic topography low in the Oligocene, now found under the Australian–Antarctic Discordance, followed by a drawing down of northern Australia as it overrode a slab burial ground now underlying much of the northern half of Australia, starting in the Miocene. Our model suggests that today's geography of Australia is strongly dependent on mantle forces. Without mantle convection, which draws Australia down by up to 300 m, nearly all of Australia's continental shelves would be exposed. We conclude that dissecting the interplay between eustasy and mantle-driven dynamic topography is critical for understanding hinterland uplift, basin subsidence, the formation and destruction of shallow epeiric seas and their facies distribution, but also for the evolution of petroleum systems.

© 2009 Elsevier B.V. All rights reserved.

1. Introduction

The motions of continents relative to large-scale patterns of mantle convection can contribute to the creation and destruction of sediment accommodation space due to transient, dynamic displacement of the surface topography, usually referred to as dynamic topography (Gurnis, 1990; Burgess and Gurnis, 1995; Lithgow-Bertelloni and

Gurnis, 1997; Gurnis et al., 1998). A significant dynamic topography effect has been demonstrated in particular for Cretaceous and Cenozoic Australian continental paleogeography based on the misfit between the global flooding patterns and the Australian continental flooding, which appears to be out-of-sync with eustasy (Russell and Gurnis, 1994; Gurnis et al., 1998; Veevers, 2001; Sandiford, 2007; DiCaprio et al., 2009). Large-scale, mantle-driven dynamic topography can be approximated by the time-dependent vertical shifts and tilts of a plane, computed from the displacement needed to reconcile the interpreted pattern of marine incursion with a predicted topography in the presence of global sea level variations (DiCaprio et al., 2009). However, some observed subsidence and uplift anomalies, particularly along the south coast of Australia (Sandiford, 2007; DiCaprio et al.,

* Corresponding author; now at StatoilHydro, Global Exploration Technology, Drammensveien 264, N-0246 Oslo, Norway.

E-mail address: christian_heine@mac.com (C. Heine).

¹ Present address: Helmholtz Centre Potsdam – GFZ German Research Centre for Geosciences, Potsdam, Germany.

2009), indicate a more complex interplay between time-dependent mantle convection and plate motion than that approximated by vertical shifts and tilts of a plane.

Geodynamic models predict between a few hundred meters and up to 2 km of surface vertical motion in response to mantle dynamic processes (Mitrovica et al., 1989; Russell and Gurnis, 1994; Lithgow-Bertelloni and Gurnis, 1997; Lithgow-Bertelloni and Silver, 1998; Gurnis et al., 1998; Conrad and Gurnis, 2003; Conrad et al., 2004; Müller et al., 2008b). Depending on the tomography model used to infer mantle density heterogeneities, Steinberger (2007) found 0.4–1.0 km rms amplitude, when converting vertical stresses to elevation beneath air, compared to 0.4–0.5 km for residual topography (i.e., observed topography corrected for crustal thickness variations and variations in ocean floor age). However, the surface expression of subducted slabs in Southeast Asia is half an order of magnitude smaller than predicted by dynamic topography models (e.g. Wheeler and White, 2000), having an upper bound of only ≈ 300 m. This has been interpreted as indication that mantle mass anomalies are supported elsewhere, presumably at internal boundaries within Earth.

Here we use a simple mantle backward-advection model to unravel the contribution of mantle convection-induced dynamic topography to the paleogeography of the Australian continent since 70 Ma. Published Australian paleogeographic and geological data are used to match modelled paleo-topography, focusing on the evolution of the large-scale spatial distribution of anomalous subsidence and uplift and to provide better constraints on the amplitudes of mantle-induced topography. Our method facilitates the quick evaluation of global and regional dynamic topography models with geological observations.

2. Australian Cenozoic paleogeography: key regions for this study

The Australian continent is characterised by vast areas of low elevation (Fig. 1), making it an excellent natural laboratory for investigating the effects of eustasy and mantle convection on paleogeography. Australia's continental margins had entered post-rift subsidence stages long before Cenozoic times (Veevers et al., 1991; Stagg et al., 1999). Rifting and breakup of the northern and western margins was completed by Late Jurassic–Early Cretaceous times, along the southern and eastern (Tasman Sea) in the Early Cretaceous and early Late Cretaceous, respectively (Gaina et al., 1998; Norvick and Smith, 2001), with thermal, post-rift subsidence commencing around 110–80 Ma (Norvick and Smith, 2001; Brown et al., 2001). The thermal effects of rifting in landward parts of marginal basins such as the Eucla Basin had likely dissipated by the beginning of the Tertiary along the central southern margin, hence can be largely disregarded for this study.

The Australian plate has undergone major changes in plate boundary forces on its northward motion throughout the Tertiary (Fig. 1b), which profoundly affected the evolution of the intraplate stress field through time, causing reactivation along pre-existing structures or weaknesses (Sandiford et al., 1995; Dyksterhuis et al., 2005; Dyksterhuis and Müller, 2008). Examples where this might have had an effect on the local topography due to significant deformation are the tectonically active Flinders/Mt. Lofty Ranges (Fig. 1; Dyksterhuis and Müller, 2008; Célerier et al., 2005; Sandiford, 2003b) and the Otway Ranges (Dyksterhuis and Müller, 2008; Sandiford 2003a,b). Collisional processes along the eastern and northern margins of the Australian plate are reported to start around Oligocene time in New Caledonia, Papua New Guinea (Cluzel et al., 2001; Schellart et al., 2006) and, later, in the New Zealand region between 25 and 20 Ma (Schellart, 2007; Kamp, 1986) and along the northern Australian margin (Hinschberger et al., 2005; Hall and Wilson, 2000; Hall, 1998). The effects from foreland loading due to orogeny prove to be negligible because of the distance from the flexural load as modelling by Müller et al. (2000b) has demonstrated. Subsidence due to changes in the far field and intraplate stress field is considered to produce elongated, asymmetric patterns (Nielsen et al.,

2007; Nielsen et al., 2005) and is not evident at the scale of this work from available Australian data. Here, we focus on subsidence and uplift anomalies at large wavelengths (1000 km and more) which cannot have their origin in structural reactivation or flexure.

The various departures of the Cenozoic Australian flooding history from global eustatic curves have been pointed out by Veevers (1984) and contributors who realised a significant misfit between continental inundation patterns and the eustatic sea level estimate of Bond (1978). Fig. 2 shows the eustatic sea level estimate of Haq and Al-Qahtani (2005) plotted versus the inundation of the Australian continent since 70 Ma. The inundation is determined by the flooded continental area relative to the present-day 200 m isobath. Whereas the eustatic sea level estimates all show a gradual decrease, the inundation of Australia increases from around 5% in early Paleocene to about 25% at present (Fig. 2).

Focusing on the Murray and Eucla Basins, the Gulf of Carpentaria and the inner parts of the North West Shelf (Fig. 1) we investigate anomalies in Cenozoic inundation patterns and their origin utilising a recent eustatic sea level curve by Haq and Al-Qahtani (2005). In middle Miocene times (<11 Ma), Veevers (1984) describes the following anomalies based on a sea level which corresponds to the present-day 20 m contour (80 m according to Haq and Al-Qahtani, 2005), assuming a constant hypsometry.

- In the Nullarbor Plain (Fig. 1), shallow marine middle Miocene limestone slopes occur from an elevation of +200 m inland towards 0 m at the coast, indicating uplift since deposition of about 180 m by tilting about a hinge near the coast. If 80 m is used as reference sea level, the inland limestone section would have been uplifted about 120 m with the coastal parts being about 50–60 m too low.
- In the Murray Basin (Fig. 1) the top of Mid-Miocene shallow marine limestone and clay has an elevation of 0 m in the east and –80 m in the west, indicating subsequent subsidence of at least 100 m about a hinge on the eastern side of the basin. Using the Haq and Al-Qahtani (2005) estimate, the deposits in the western part must have subsided about 160 m.
- The Lake Eyre region (Fig. 1), today at 12 m below sea level, was not covered by the Miocene sea which rose +20 m (or +80 m according to Haq and Al-Qahtani, 2005) above the present sea level. The top of the Miocene lacustrine–fluvial Etadunna Formation is today found at –17 m implying subsidence of about 40 m or 100 m using Haq and Al-Qahtani (2005).
- In the Cape Range area (Fig. 1) of Western Australia's onshore Carnarvon Basin, Mid-Miocene shallow marine limestone is now found at elevations of +300 m, implying local uplift of 280 m (220 m, Haq and Al-Qahtani, 2005) since deposition.

For the Eocene–Miocene times (38–24 Ma), Veevers (1984) assumes a sea level of 75 m above present (Bond, 1978), whereas the work of Haq and Al-Qahtani (2005) indicates a sea level of 220–180 m for this time:

- In southwestern Australia, Late Eocene shallow marine sediments now have an elevation of +250 m near Norseman, resulting in a net uplift of 175 m (Haq and Al-Qahtani, 2005). At the northern edge of Eucla Basin, along the western and north-eastern margins and off north-eastern Queensland, the Eocene and Miocene shorelines coincide, indicating a subsidence of 55 m (Haq curve: 100–140 m) in the Oligocene.
- In the Lake Eyre area, the top of the Eocene non-marine Eyre Formation has an elevation of –60 m, implying subsidence of at least 135 m (240–280 m) since the Eocene, comprising at least 60 m in the Oligocene (Veevers, 1984).
- In the Renmark area of the Murray Basin, the top of the Late Eocene shallow marine clay has an elevation of –200 m, indicating 275 m (≈ 380 –420 m) of subsidence since the Eocene.

In summary, there are numerous localities along the Australian continental margins and in the interior where eustatic sea level variations and local tectonics alone cannot explain the large-scale

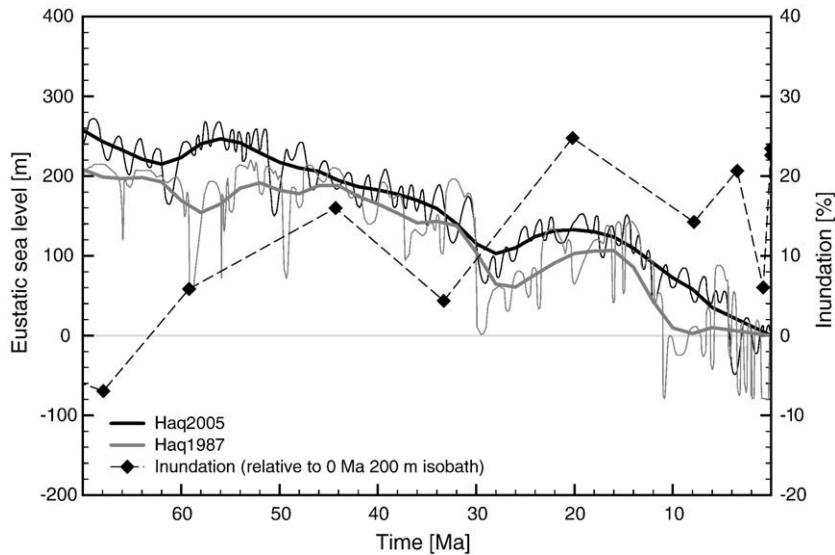


Fig. 2. Global eustatic sea level curves and inundation history of the Australian continent based on paleoshorelines derived from Langford et al. (1995). Solid black curves based on Haq and Al-Qahtani's (2005) sea level curve, with thin line representing the original estimate, thick line: filtered curve. Solid gray curves are based on Haq et al.'s (1987) sea level curve, with thin line representing original curve, thick line filtered curve. Filtered lines show long-wavelength component of the eustatic sea level estimate using a cosine arch filter with 10 m.y. window. The amount of inundation is computed relative to the present-day 200 m isobath derived from the ETOPO2 global 2' topography (N.O.A.A., National Geophysical Data Center, 2006).

3. Methodology

3.1. Mantle convection and dynamic topography model

Seismic tomography captures information about the present-day distribution of materials that produce fast and slow perturbations to a reference Earth velocity model. Velocity variations relate to both thermal and compositional variations, both of which affect buoyancy. Commonly it is assumed that relatively higher seismic velocities indicate colder material downwelling whereas areas of lower seismic velocities indicate hotter material upwelling (Grand et al., 1997; van der Hilst et al., 1997).

Using a well established global mantle-convection modelling approach, we compute the time-dependent surface topography for the last 70 Myrs by advecting density anomalies back in the mantle flow field (Xie et al., 2006; Steinberger et al., 2004). We use a global, self-consistent plate kinematic model (Müller et al., 2008a), based on a moving hotspot absolute plate motion reference frame (O'Neill et al., 2003), to impose surface plate motion constraints on the mantle-convection model. Relative density anomalies are derived by converting relative seismic velocities from the global S20RTS seismic tomographic model (Ritsema et al., 1999) using an empirical conversion factor of 0.25 below depths of 220 km. This velocity-to-density scaling factor is based on a good fit with the observed geoid and consistent with mineral physics (Karato, 1993; Steinberger and Calderwood, 2006). We assume that both seismic velocity and density anomalies in the sub-lithospheric mantle are due to temperature changes, and hence perfectly correlated.

According to the isopycnic hypothesis, seismic velocity variations in the continental lithosphere do not correspond to density variations, or correspond to only very small density variations (Jordan, 1978, 1988; Shapiro et al. 1999). Excluding a heterogeneous lithosphere (upper 220 km) thus avoids gross overestimation of dynamic topography amplitudes (Steinberger et al., 2001). However, parts of the Australian lithosphere indicate that deep lithospheric keels and potential compositional heterogeneities might extend deeper than 220 km (Fishwick et al., 2008; Artemieva, 2003) and be responsible for over-prediction of the dynamic topography amplitude. Conversely, in regions near the coast or in southeastern Australia, where the lithosphere is thin, calculations would probably be more accurate if

some velocity perturbations shallower than 220 km were used as well.

The flow field of the mantle for the last 70 Ma is calculated using a spectral method (Hager and O'Connell, 1981), by spherical harmonic expansion of surface plate velocities and internal density heterogeneities at each depth level (Steinberger et al., 2004; Xie et al., 2006; Steinberger and Calderwood, 2006). The viscosity model (Steinberger et al., 2004) considers only radial viscosity variations and is based on mineral physics and yields a good fit globally with the geoid and other observations. The model is constrained by matching paleo-latitudes of hotspots from paleomagnetic data and geometry and age progression along hotspot tracks. The change of mantle density anomalies with time is computed by advecting them back in the mantle flow field through time as a function of their buoyancy (Steinberger et al., 2004). The backward advection has been modified by (a) always continuing backward advected upwellings up to 220 km at each time step, thus improving the restoration of past mantle upwellings, and (b) removing backward-advected downwellings in the uppermost 220 km (Müller et al., 2008b).

From the backward-advected density models, the vertical stress at the upper boundary is computed. Here a horizontal stress-free boundary condition is used on the upper boundary of the high-viscosity lithosphere (2.4×10^{22} Pas). Vertical stresses are converted to topography with a density contrast of 3.3 g/cm^3 . That means, the dynamic topography computed here is appropriate for "beneath air" but this "raw" dynamic topography is "downscaled" using an empirical factor (see section 3.4).

The model output is relative to the geoid (i.e. relative to sea level). We limit our backward-advected models to the past 70 Myrs, which is about the time span for which mid-mantle structure can be reconstructed reasonably well using a backward-advection analytical flow model.

3.2. Eustatic sea level estimates

Long-term fluctuations of the global sea level through geological time are primarily caused by changes in the volume of the ocean basins and fluctuating inland ice volume. These have long been recognised through their effect on depositional patterns on continental platforms and margins (Bond, 1978; Hallam, 1984; Watts and Thorne, 1984; Haq

et al., 1987; Sahagian and Watts, 1991; Sahagian and Jones, 1993; Miller et al., 2005). Eustasy provides an important constraint for modelling epeirogenic and tectonic motion from flooding patterns. Over the past 30 years several attempts have been made to generate eustatic sea level curves (Müller et al., 2008b; Haq and Al-Qahtani, 2005; Haq et al., 1987; Miller et al., 2005; Sahagian et al., 1996) with little consensus reached up to the mid 1990's (Miall, 1992; Christie-Blick and Driscoll, 1995).

Recent work estimating the eustatic sea level through computing the volume of ocean basins through time in combination with dynamic topography models (Müller et al., 2008b) suggests that eustatic sea level estimates based on the New Jersey margin (Miller et al., 2005; Watts and Thorne, 1984) are significantly underestimated, due to the effect of mantle-driven dynamic topography on the east coast of North America during the Tertiary (Spasojević et al., 2008; Müller et al., 2008b). Müller et al. (2008b) demonstrated that the eustatic sea level amplitudes and long-time trend based on ocean basin volume changes are similar to Haq and Al-Qahtani's (2005) curve (Fig. 2). We have hence chosen the latter curve as eustatic sea level input for our models. The Haq and Al-Qahtani's (2005) curve represents an updated version of the original Meso- and Cenozoic eustatic sea level chronology (Haq et al., 1987), recalibrated to the numerical Geologic Time Scale 2004 (Gradstein et al., 2004).

3.3. Paleogeographic data and sedimentation

Digital paleogeographic maps from *The Paleogeographic Atlas of Australia – Vol. 10 Cainozoic* (Langford et al., 1995) were used to empirically scale the dynamic topography input to optimise the agreement between modelled and observed paleo-topography, as explained in Section 4. The compilation of Langford et al. (1995) contains geological data for the Cenozoic which are averaged for individual time slices (Supplementary material, Table 1). Struckmeyer and Brown (1990) interpreted the depositional environment of a total of 361 datapoints, providing the base for Langford et al.'s (1995) work who grouped the date into digital sets of georeferenced polygons, according to broad paleo-environment characteristics (e.g. “land erosional” or “marine shallow”). We have combined all polygons classified as “land” to reconstruct a coherent continent-wide paleo-shoreline for each time slice to derive the amount of flooding. We excluded time slices 7 (Pleistocene) and 8 (Holocene) due to the spatio-temporal resolution of our model. It is important to remark that the data from Langford et al. (1995) represent the maximum extent of a distinct paleogeographic environment integrated over each given time interval. Ages from the paleogeographic atlas are based on the Berggren et al. (1995) time scale. These were converted to the GTS2004 time scale (Gradstein et al., 2004). We accounted for sediment deposition by backstripping the sediments at available datapoints (Langford et al., 1995) and isostatically correcting the topographic base level of our model. The backstripping technique, as outlined by Steckler and Watts (1978), is used to isolate the effects of sediment loading from the tectonic subsidence of the basement by restoring and subsequently removing the decompacted sediment thickness at time of deposition (Allen and Allen, 2005; Slater and Christie, 1980):

$$Y = S \frac{\rho_m - \bar{\rho}_s}{\rho_m - \rho_w} \quad (1)$$

where Y is the isostatic correction, ρ_m and ρ_w are the densities of mantle rocks and water, respectively, S is the thickness of the decompacted sedimentary unit, and $\bar{\rho}_s$ is the average density for the sedimentary unit. Local 1D backstripping was applied to each datapoint to account for sediment deposition and to restore the appropriate surface elevation using Airy isostasy.

Due to relatively thin Cenozoic sediment thicknesses, large regional extent of the deposits, and high elastic thickness values of the Australian lithosphere (Swain and Kirby, 2006; Simons and van der Hilst, 2002),

flexural effects from sedimentary loading are negligible and Airy-type compensation can be assumed. The individual datapoints with decompacted sections were gridded for the individual time slices using a continuous curvature fitting gridding algorithm (Wessel and Smith, 1998). It is assumed that elevations above the present-day 300 m contour have been dominantly erosional with insignificant amounts of sediment being deposited.

In areas without hydrocarbon prospectivity, most of the Cenozoic datapoints lack accurate stratigraphic thickness information for individual time steps. The absence of coherent sequence stratigraphic frameworks for the onshore Cenozoic in Australia, for example the Eucla Basin (Clarke et al., 2003) might have complicated the regional data compilation and could be one cause for erroneous stratigraphic interval information. We have checked the values reported by Langford et al. (1995) against the Geoscience Australia National Petroleum wells database (<http://dbforms.ga.gov.au/www/npm.well.search>, accessed 2009-02-10) and published stratigraphic data for the locations used for backstripping and topographic modelling (Figs. 6 and 7).

3.4. Methodology, model calibration, and scaling

We assume that the present-day topography of Australia (Fig. 3a, Sandwell, 2009) contains mantle-driven topography components, which are represented by our dynamic topography model for the present (Fig. 3b). To obtain a topography without mantle-driven components as base grid (Fig. 3c), we subtract the present-day dynamic topography signal from the digital elevation model (DEM) of Australia. Subsequently, dynamic topography models for the last 70 Myrs are rotated into the fixed present-day Australian position using the EarthByte rotation model (Müller et al., 2008a) and merged with the “non-dynamic” base DEM grid. The procedure is repeated in 1 m.y. intervals, effectively evaluating the difference between dynamic topography estimates between the time steps. Sediment-unloading corrections are applied to the surface elevation estimates for the Australian region to account for sediment deposition through time. The eustatic sea level estimate for any given time is then added to the grid to obtain a paleo-DEM.

The paleo-shoreline positions derived from the environment-polygons of (Langford et al., 1995) are then used to achieve a best-fit match of the reconstructed paleogeography by empirically scaling the dynamic topography model output grids using an iterative approach. A series of reconstructions for a range of scaling factors was made and their fit analysed over the 70 timesteps. Most weight has been assigned to the fit with paleogeographic data in low-lying regions which have been tectonically stable over the last 70 Myrs, having recorded transgressive and regressive cycles in the sedimentation record. These were the Murray Basin, the Eucla Basin, the Gulf of Carpentaria and parts of the North West Shelf. Most emphasis was put on a regional evaluation of a best fit, i.e. matching general patterns of regression and transgression, and flooding and uplift over the entire Australian region rather than attempting to fit individual key sections. However, it is important to note that in areas of low topographic gradients, our predicted shoreline position is highly susceptible to errors as little changes in elevation here will result in large changes in the coastline location.

An empirical scaling factor of 0.55 for the dynamic topography model was found to yield the best match between the paleogeographic data and modelled flooding patterns on continent-scale. The necessity for downscaling the raw dynamic topography field probably primarily reflects shortcomings of the currently used conversion of mantle seismic shear-wave velocities to density anomalies:

1. Not all seismic velocities variations below 220 km are of thermal origin. In the current analytical approach all seismic shear-wave velocity anomalies are converted to density anomalies with the

same conversion factor corresponding to thermal anomalies. However, the existence of chemical heterogeneities, especially in the lower mantle, has clearly been demonstrated (Trampert et al., 2004). Therefore, using a thermal scaling factor may not always be appropriate. In areas with a thick tectosphere, seismic velocity anomalies in the upper mantle might also be related to chemical boundary layers and compositional heterogeneities extending deeper than 220 km (Shapiro et al., 1999). This is probably the case for some parts of the Australian lithosphere (Fishwick et al., 2005; Fishwick et al., 2008; Stoddard and Abbot, 1996).

- Further, the procedure of backward-advecting converted seismic velocity anomalies through time yields potential problems as it does not account for heat diffusion. A shallow negative seismic anomaly, for example, is computed to occur at greater depths back through time, causing less dynamic topography in the past. In reality, this would have occurred only if the associated upwelling had only recently arrived beneath the lithosphere. If the upwelling had been there for longer time it might have been stronger in the past, which would, to the contrary of what is computed in the model, result in dynamic subsidence (Xie et al., 2006). Hence, dynamic topography and its changes through time are difficult to predict from backward-advection models and the results should be treated with the appropriate caution.

In addition, predicted dynamic topography depends on viscosity structure, which is uncertain. The structure adopted here is meant to represent a global average, yet regional variations almost certainly exist. In particular, it is not well known how pronounced a low-viscosity asthenosphere there is beneath Australia, i.e. how thick it is and what is the minimum viscosity. Also, some viscous stresses may be supported on deep interfaces (Wheeler and White, 2000). The nature of such interfaces is currently unknown, and including the main known phase boundaries with their experimentally determined parameters has been shown to be insufficient to achieve a sufficiently substantial reduction in dynamic topography (Steinberger, 2007). Hence the additional scaling factor may also be viewed as an “ad hoc” implementation of the effect of unknown deep interfaces.

4. Modelling Australia's Cenozoic paleogeography

By combining results from topographic reconstructions using the eustatic sea level variations, dynamic topography and plate kinematics, the effects of mantle dynamics on the paleogeography can be clearly demonstrated. Throughout the Cenozoic, dynamic topography has had considerable impact on the inundation history of the Australian continent. The mantle convection-induced surface deflection resulted in a transient, complex dynamic warping of the region. Comparing the modelling results with published paleogeographic maps, it is possible to correlate large-scale patterns of dynamic up- and downwelling with areas of uplift or subsidence on the Australian continent.

4.1. Paleocene–Early Eocene (66.4–52 Ma)

Paleogeographic data for the Paleocene–Early Eocene suggest that the Australian region was mostly emergent above sea level and that the Latest Cretaceous/Early Paleocene coastline lay well seaward beyond the present-day coastline (McGowran et al., 2004; Veevers, 2001; Langford et al., 1995), although eustatic sea levels fluctuated around 220 m above the present level (Haq and Al-Qahtani, 2005).

Our dynamic topography models suggest that from the beginning of the Paleocene to Early Eocene, Australia gradually moved over a dynamic topography low situated below the northwestern half of the continent, due to slow (36 mm/yr) northwestward absolute motion of Australia from 65 to 45 Ma (Whittaker et al., 2007). The low has a minimum amplitude of around –150 m at 61 Ma. The southwestern part and eastern half of the Australian continent are predicted to be affected

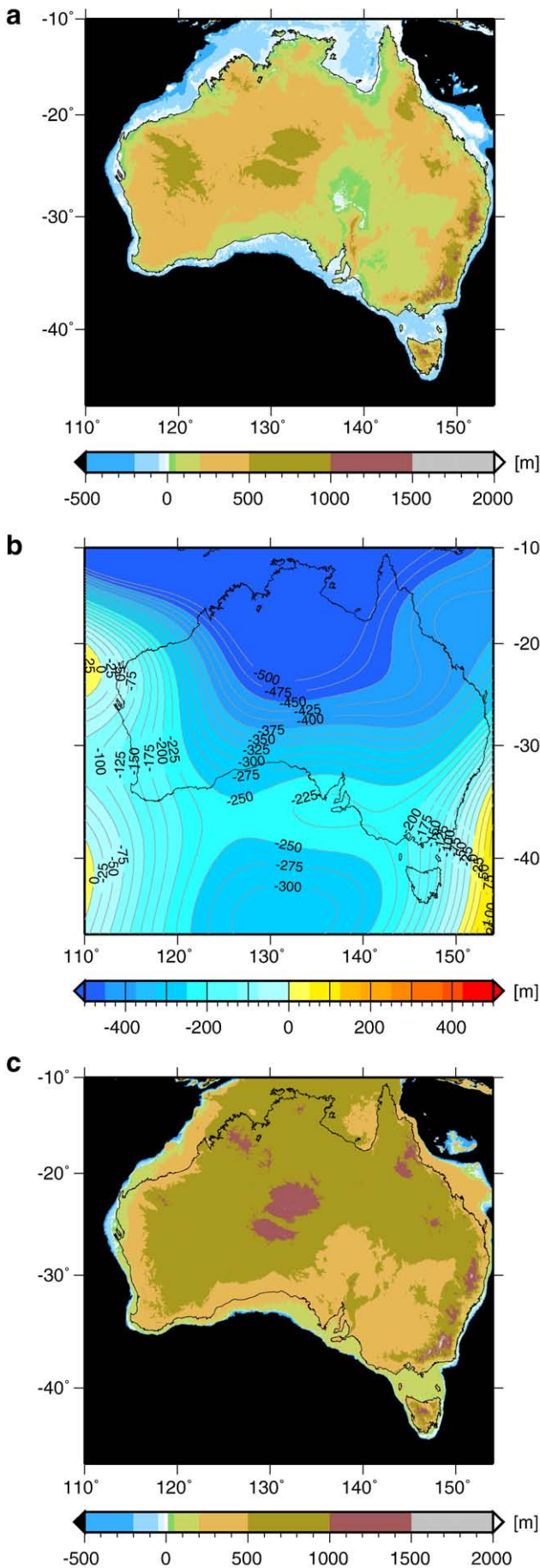
by positive dynamic topography, with a regional high situated below southeastern Australia having an amplitude of up to 150 m (Fig. 4a).

The paleo-DEM for the Paleocene largely corresponds to the geological observations along the western, southern and eastern segments of the margin, with major mismatches in northern Australia (Fig. 4a). Our modelled topography for the North West Shelf margin shows slightly overestimated water depths (50–100 m), resulting in a more landward position of the shoreline as compared to Langford et al. (1995). In the Great Australian Bight, predicted water depths are overestimated with the model shoreline located significantly landward with respect to the reported shoreline during this interval, however, northern parts of the Eucla Basin are modelled as exposed in accordance with observations (Hou et al., 2006; Hou et al., 2008). The Murray Basin is modelled as southward dipping, low-lying depression, suggesting a good fit with an observed depositional fluvio-lacustrine/marginal marine environment where the sand- and claystones and interbedded coals of the Renmark group cover Pre-Tertiary basement (Roy et al., 2000; Langford et al., 1995; Veevers, 1984). The Gulf of Carpentaria is modelled as subaerially exposed at elevations of around 200–300 m, forming a broad northward trending depression. Paleogeographic data indicate a large, low-lying fluvial depositional system occupying the Gulf of Carpentaria region, opening northwards into the proto-Arafura Sea. Along the northern margin our model overestimates elevations compared to reported paleo-shoreline positions. We relate this to the poor sediment thickness data coverage in this frontier region, resulting in an underestimation of the computed isostatic correction.

4.2. Middle–Late Eocene (52–36.6 Ma)

A circum-Pacific plate tectonic reorganisation in Early Eocene times caused a change in plate motion direction for the Australian plate from NW to NNE and dramatic increase in plate velocity to around 48 mm/yr relative to the underlying mantle (Whittaker et al., 2007; Müller et al., 2000a). The center of the modelled dynamic topography low is shifted below central Australia/Eucla Basin and amplitudes increased to around –200 m (Fig. 4b). Contemporaneously, predicted dynamic topography amplitudes in the eastern and southeastern parts of the Australian region decrease by around 50–100 m, whereas our model suggests a \approx 200 m uplift of the North West Shelf region due to dynamic topography. Eustatic sea level lowered and fluctuated around 200 m (Fig. 2).

In the Gulf of Carpentaria observations indicate a retreat of the coastlines southwards, generating broad floodplains (Langford et al., 1995). Our modelled paleogeography for the Eocene (43 Ma; Fig. 4b) shows a near-circular depression of the central Gulf of Carpentaria region with elevations below 50 m. The modelled topography is generally over-predicted (cf. Section 4.1) positioning the modelled coastline significantly too far north. Along the North West Shelf observed shorelines still lie well outboard of the present-day coastline, except in the Carnarvon Basin where the present-day onshore parts are flooded, which is well predicted by our paleo-elevation model. Along the western, southwestern and eastern Australian margins, including the Queensland Plateau, geological data indicate coastline positions well outboard of the present-day coastline which is matched by our model (Fig. 4b). In most parts of the Great Australian Bight margin we overestimate elevations with the coastline being modelled max. 500 km too far oceanward and most of the Eucla Basin as subaerially exposed. Here, sediments indicate a dramatic transgression, flooding nearly all of the present-day Eucla Basin up to its northern margin (de Broekert and Sandiford, 2005; Langford et al., 1995). The modelled topography for the Eucla Basin, however, is below 50 m. Similarly to the Gulf of Carpentaria, the accuracy of sediment thickness data in this frontier region will have significant effects on the model outcome. In the Murray Basin, the model yields a reasonable fit with the observations, indicating large areas below 10 m elevation. This is well in agreement with the observation of a minor marine inundation and deposition of shallow marine and



marginal marine/lacustrine sediments (Roy et al., 2000). In the Lake Eyre region, non-marine units of the Eyre Formation are deposited (Veevers, 2001; Langford et al., 1995).

4.3. Late Eocene–Early Oligocene (36.6–30 Ma)

During the Late Eocene–Oligocene time Australia continued to move northwards toward the SE Asian subduction zone system at high velocities of around 68 mm/yr (Fig. 4c). Our model indicates that the leading northern edge of the Australian plate became increasingly affected by increasing negative dynamic topography, placing the Gulf of Carpentaria and York Peninsula over the Melanesian slab burial ground. Amplitudes of the dynamic topography low beneath the Eucla basin increase to around -250 m leading to the development of an E–W striking arch of lower negative dynamic topography across Australia (Fig. 4c).

The Early Oligocene is characterised by a sea level lowstand at upper Early Oligocene times. Shorelines retreat to the outer continental shelf all around the continent as indicated by unconformities (Langford et al., 1995), and climatic conditions change in response to the opening of a marine gateway between Tasmania and Antarctica (e.g. Müller et al., 2000a; Royer and Rollet, 1997). Our Early Oligocene Paleo-DEM indicates good fits between predicted and observed location of the paleo-shorelines along the North West Shelf, western margin, southeastern (Bass Strait) and eastern margins (Fig. 4c). Shallow marine to fluvial conditions (Duddy, 2003; Langford et al., 1995) in the Murray Basin are correctly predicted, as well as exposure of the Gulf of Carpentaria above sea level. In the Great Australian Bight, our predicted shoreline is situated significantly further landward than the one reported by Langford et al. (1995), with observations indicating erosion and a shift of depocenters basinward into the Great Australian Bight (Hou et al., 2008; Hou et al., 2006).

4.4. Late Oligocene–Late Middle Miocene (30–10.4 Ma)

Fast northward motion of Australia continued in the Early/Mid-Miocene. We predict that the entire northern half of the continent was affected by increasing negative dynamic topography related to the SE Asian subduction zone system (Fig. 4d) during this time. Modelled amplitudes in the northern parts of Australia reach up to -450 m, while the southern downwelling progressively affects areas south of the continental margin. The western margin is situated parallel to the zero dynamic topography contour, while southern Australia is placed over an E–W elongated band of less pronounced mantle downwelling.

A global sea level rise from the Early Oligocene to the Early Eocene (Fig. 2) resulted in a marine transgression in the Late Oligocene, leading to a widespread deposition of shallow marine limestones and flooding of the marginal basins around Australia in the Miocene (Langford et al., 1995). Modelled paleo-shorelines at 15 Ma (Early/Mid-Miocene) match Langford et al. (1995)'s interpretation well along the North West Shelf, the western margin, the southeastern and eastern margins (Fig. 4d). We over-predict elevations in the Eucla Basin, which was inundated during the Latest Oligocene until the Mid-Miocene, and the northern margin off the Northern Territory, resulting in modelled subaerial exposure where shallow marine conditions are reported (Langford et al., 1995). Flooding along the southern parts of the Carpentaria Basin is also over-predicted, causing our modelled paleo-shoreline to be located too far landward. In the Murray Basin our predicted elevation agrees with the reported deposition of shallow marine/epicontinental limestones (McGowran et al., 2004; Lukasik and James, 2003).

Fig. 3. Present-day Australian topography, dynamic topography and difference topography. (a) present-day surface topography; (b) scaled dynamic topography; (c) DEM with dynamic topography component subtracted, which is used as base grid for topography reconstructions. Thin, black line is present-day coastline.

4.5. Late Miocene (10.4–5.3 Ma)

The continued northward motion of the Australian continent at relatively high plate velocities towards the SE Asian slab burial ground resulted in further increase of the area affected by negative dynamic

topography along Australia's northern margin (Fig. 4e). At this time, we predict that nearly all of Australia is affected by downward-deflection of the surface topography due to mantle convection. The E–W striking arch of less negative topography straddles the southernmost Australian margin and dynamic topography amplitudes reach 550 m in

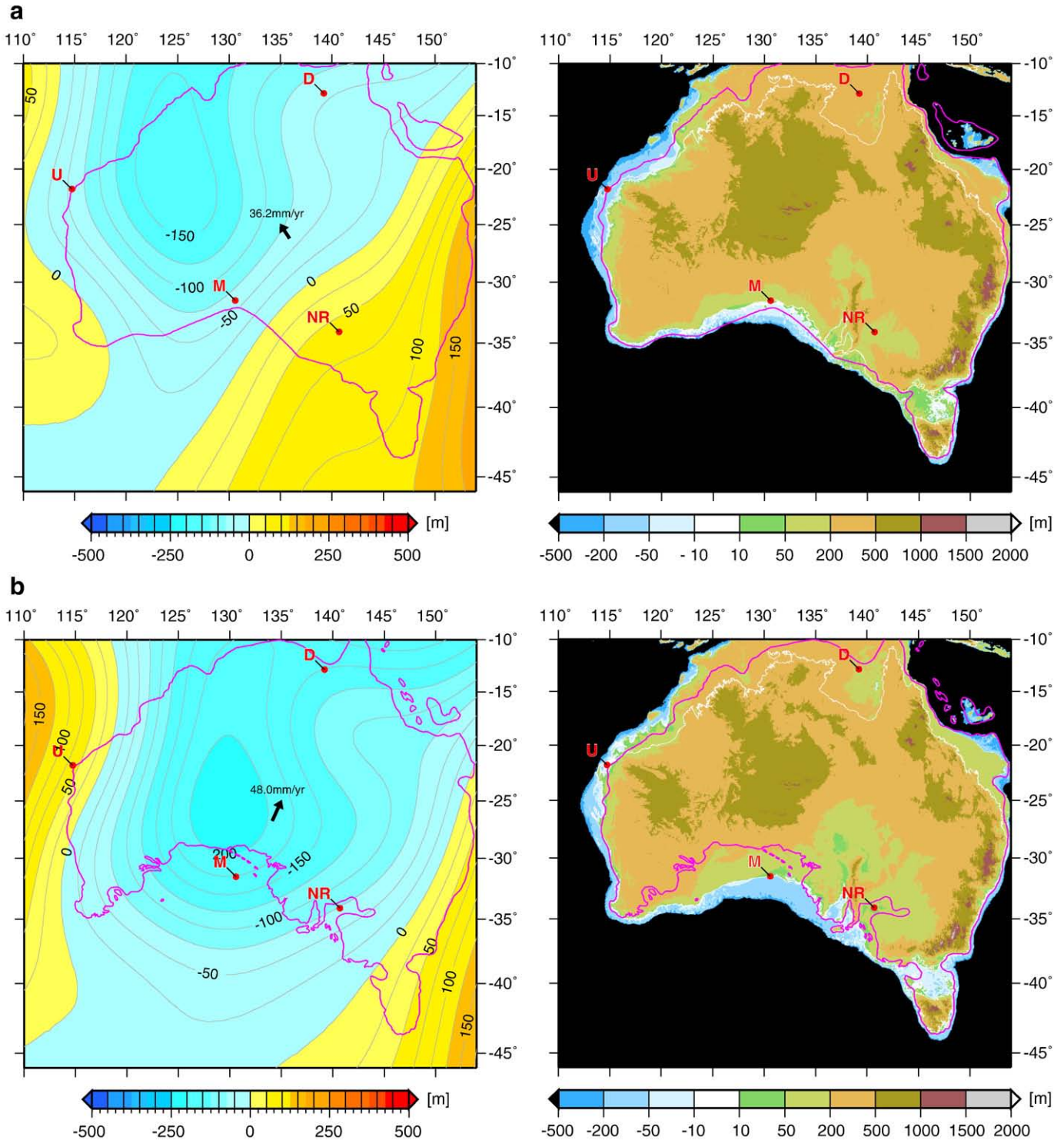


Fig. 4. Dynamic topography and best-fit paleogeographic reconstructions, combining dynamic topography models, eustatic sea level variations and isostatic correction for sediments for six different times. Eustatic sea level is based on Haq and Al-Qahtani (2005) and isostatic correction uses sediment thickness based on well data from Langford et al. (1995). a) ≈ 61 Ma (Early Paleocene, Cenozoic 1 interval); b) ≈ 43 Ma (Mid Eocene, Cenozoic 2 interval); c) ≈ 32 Ma (Early Oligocene, Cenozoic 3 interval); d) ≈ 15 Ma (Mid Miocene, Cenozoic 4 interval); e) ≈ 8 Ma (Late Miocene, Cenozoic 5 interval); f) ≈ 3 Ma (Pliocene, Cenozoic 6 interval). Australia is kept fixed in present-day coordinates. Magenta-coloured line indicates paleo-shoreline position based on the combined interpreted “land” environments (Langford et al., 1995) for each individual time slice. Red dots indicate wells for which a modelled elevation history is shown in Fig. 7.

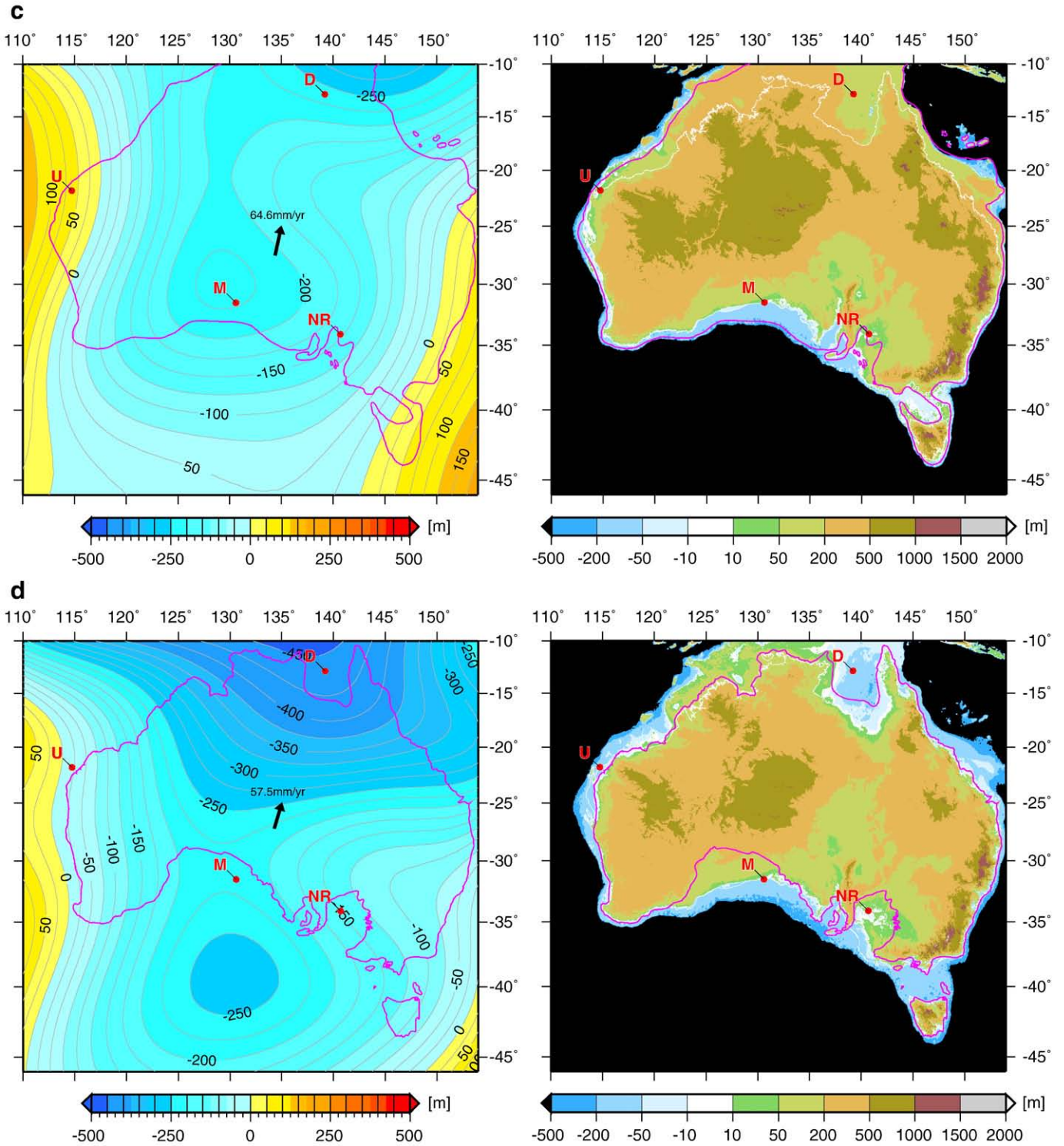


Fig. 4 (continued).

northern Australia and around -200 to 250 m along the southern margins (Fig. 4e).

Further lowering of global eustatic sea level in the Late Miocene resulted in a repeated regression along most of the continental shelf and marginal basins similar to that in the Early Oligocene (Langford et al., 1995). Our predicted topography for the Late Miocene (at 8 Ma) largely agrees with paleogeographic data along the northwestern, western and southeastern margins of Australia (Fig. 4e). The topography of the

Murray Basin is modelled as semicircular depression elevated 10 – 50 m above sea level, in accordance with a Mid-Late Miocene unconformity (Gallagher and Gourley, 2007). We predict too deep bathymetry for the southern Gulf of Carpentaria, the northernmost margin, the Bight margin and the northeastern margin, resulting in the modelled paleoshorelines being located too far landward. Along the northern margin, the onset of the collision of the northern Australian margin with the Sunda Trench (Hall, 2002) and the associated flexural response

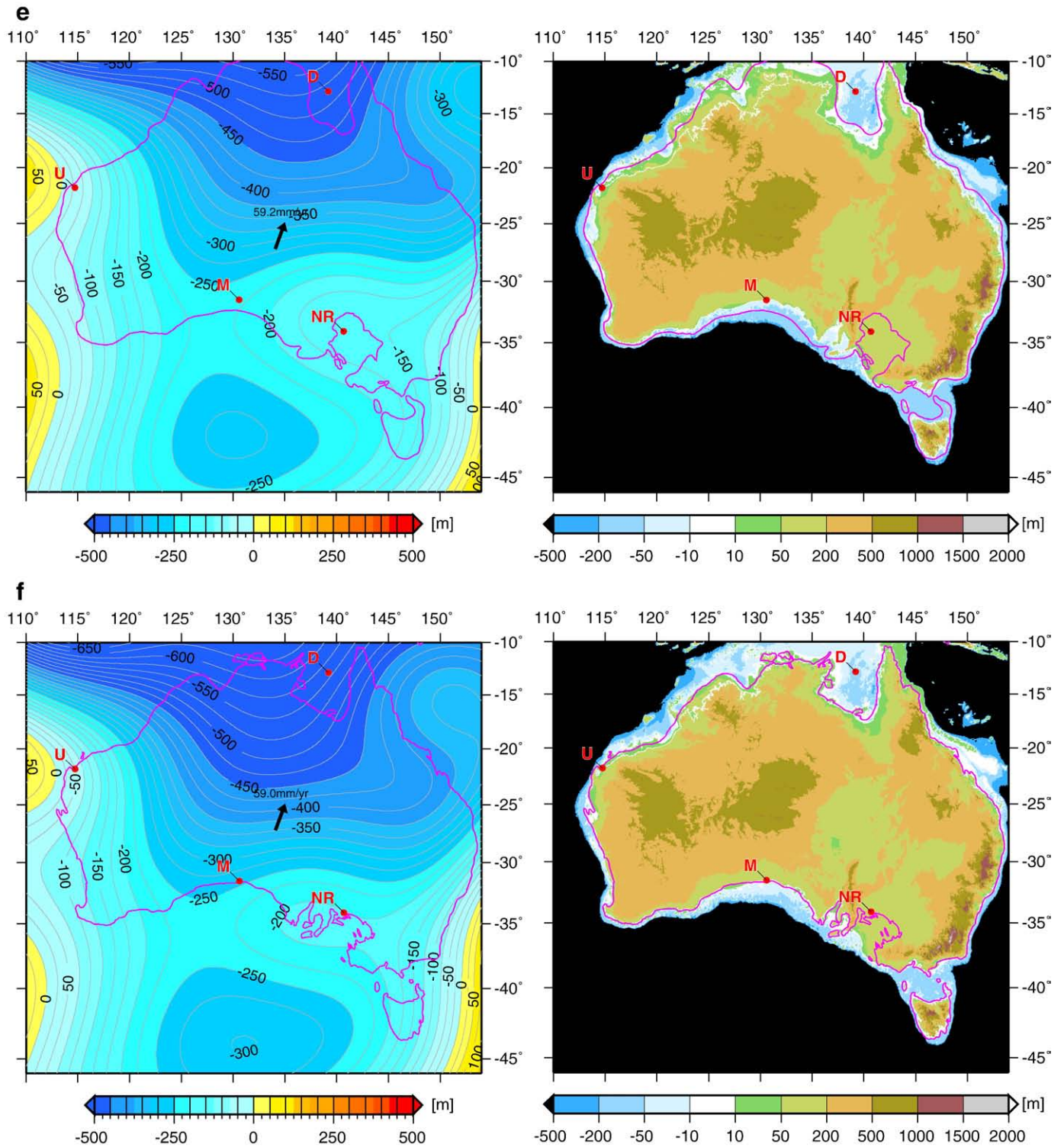


Fig. 4 (continued).

(Harrowfield and Keep, 2005) might have overprinted any signature from dynamic topography and eustatic sea level changes.

4.6. Pliocene (5.3–1.6 Ma)

Collision along the northern Australian plate margin with the subduction zone arc system of SE Asia had already commenced during the Miocene (Hall, 2002). Our modelled dynamic topography for the Pliocene time slice is characterised by further increase in negative

amplitudes for the northern to central parts of the continent as northward motions at relatively high velocities continue (Fig. 4f). Predicted amplitudes increased to around 600 m along the northern margin. However, the dynamic topography with amplitudes of around 250 m along the southern margin did not change markedly since 15 Ma.

The gradual change from the Late Miocene to Pliocene paleogeography is well reflected in our predicted topography of the Australian continent at 3 Ma (Fig. 4f). There is broad agreement between our

modelled and the interpreted paleo-shorelines (Langford et al., 1995) along all continental margins and most marginal basins. We overestimate the topography of the Murray Basin by 10–50 m as indicated by a rapid marine transgression and subsequent deposition of shallow marine muds and barrier sand complexes in the southwestern and central parts of the basin (Langford et al., 1995; Roy et al., 2000). Fishwick et al. (2005), Finn et al. (2005), and Simons et al. (1999) suggest a thin lithosphere which is altered and infiltrated by volatiles due to subduction along the Australian Pacific margin and opening of the Tasman Sea in the late Cretaceous (Gaina et al., 1998). These

heterogeneities occur above our 220 km depth model-cutoff and hence might not have been appropriately accounted for (cf. Section 3.1).

5. Vertical motions of the Australian continent

By combining dynamic topography models with eustatic sea level variations and local tectonic subsidence analysis based on published well data, the vertical motions of the Australian continent can be estimated. We have modelled the elevation history of four different wells situated in low elevations on the passive margins or in close

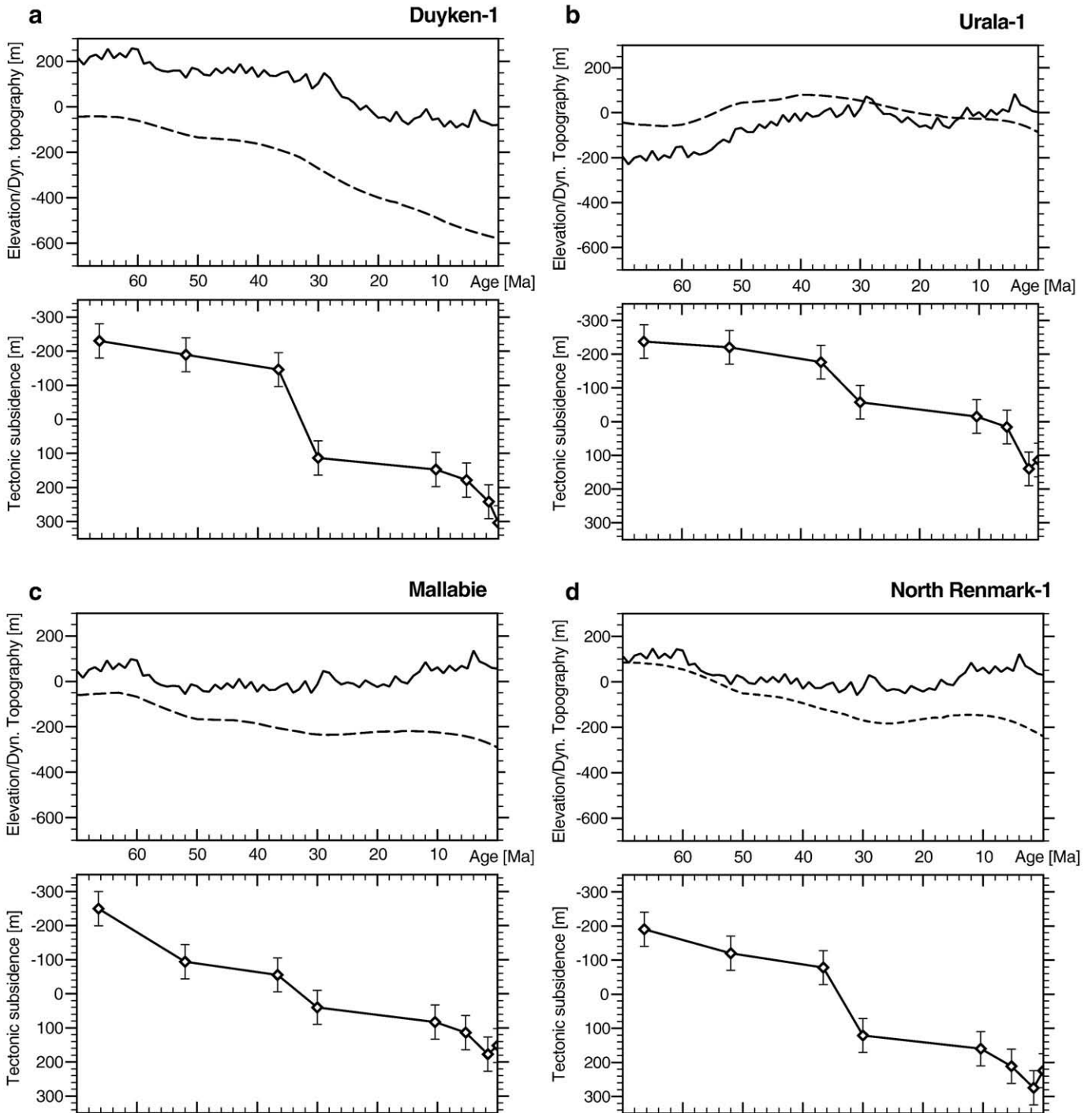


Fig. 5. Scaled dynamic topography (upper plots, dashed line), reconstructed topography histories relative to sea level (upper plots, solid line), and tectonic subsidence adjusted for eustatic sea level (lower plot, solid line) for 4 selected wells for the last 70 Ma. (a) Duyken-1 well, Carpentaria Basin; (b) Urala-1 well, North Carnarvon Basin; (c) Mallabie well, eastern Eucla basin; (d) North Renmark-1 well, Murray Basin. Error bars in lower plots mark ± 50 m uncertainty in paleowater depth. For location of the wells see Fig. 6.

vicinity, located in the Gulf of Carpentaria, the North West Shelf, the Eucla and Murray Basins.

The tectonic subsidence of the Carpentaria Basin, represented by the Duyken-1 well (Fig. 5a), exhibits gradual tectonic subsidence throughout the Tertiary, punctuated by a rapid subsidence pulse between 36 and 30 Ma. The gradual background tectonic subsidence throughout the Tertiary is unexpected for this old epicratonic basin without taking mantle dynamics into account – no significant thermal subsidence during the Tertiary is expected. According to our mantle-convection model, this area has experienced continued slow subsidence during the Tertiary (Fig. 5a), roughly matching the observed tectonic subsidence in this area if we exclude the sharp subsidence pulse between 38 and 30 Ma, thus providing a favourable match between observations and model. The cause for the rapid subsidence pulse is enigmatic as the onset of collision processes in Papua New Guinea only starts in Mid-Oligocene times.

The Carnarvon Basin is well known to show anomalous, gradual accelerated tectonic subsidence in the Late Tertiary (Müller et al., 2000b), even though it is located over 1000 km away from the Sunda Trench, ruling out flexural plate bending influence on tectonic subsidence. The last rifting episode affecting the region was the India–Australia breakup in early Cretaceous times (Exon and Colwell, 1994). Well Urala-1 in the Carnarvon Basin shows accelerated tectonic subsidence after 36 Ma in the order of 300 m (Fig. 5b). Our dynamic topography model predicts about 200 m of subsidence for

this location (Fig. 5b), originating from the growing influence of the slab material sinking underneath northern Australia during this time period (Fig. 4c), as Australia continues to move towards the Melanesian subduction system at speeds over 60 mm/yr (Fig. 4a–c).

In the eastern onshore Eucla Basin, the Mallabie-1 well also shows continuous tectonic subsidence over the past 70 Ma with a minor phase of accelerated subsidence between 36 and 30 Ma (Fig. 5c). The well is located in the vicinity to the southern Australian passive margin and hence was subtly affected by the rifting between Australia and Antarctica (Brown et al., 2001). We interpret the subsidence until 36 Ma to be dominated by decaying thermal subsidence related to the Australia–Antarctica breakup. However, the observed continued tectonic subsidence (Fig. 5c) in post-Eocene times points towards anomalous subsidence. Our modelled dynamic topography for the period between 36 Ma and present-day indicates the generation of about 100 m of additional accommodation space due to mantle effects.

The Murray basin (North Renmark-1 well, Fig. 5d) exhibits gradual tectonic subsidence totalling about 100 m, from 66 to 37 Ma, even though this area is not known to have experienced any crustal thinning during the rift-phase between Australia and Antarctica – the Murray basin is merely an intracontinental area inundated by shallow seas at various times during the Tertiary (Lukasik et al., 2000). This raises the question why it should display tectonic subsidence during the Early Tertiary. A strong, accelerated subsidence pulse of nearly

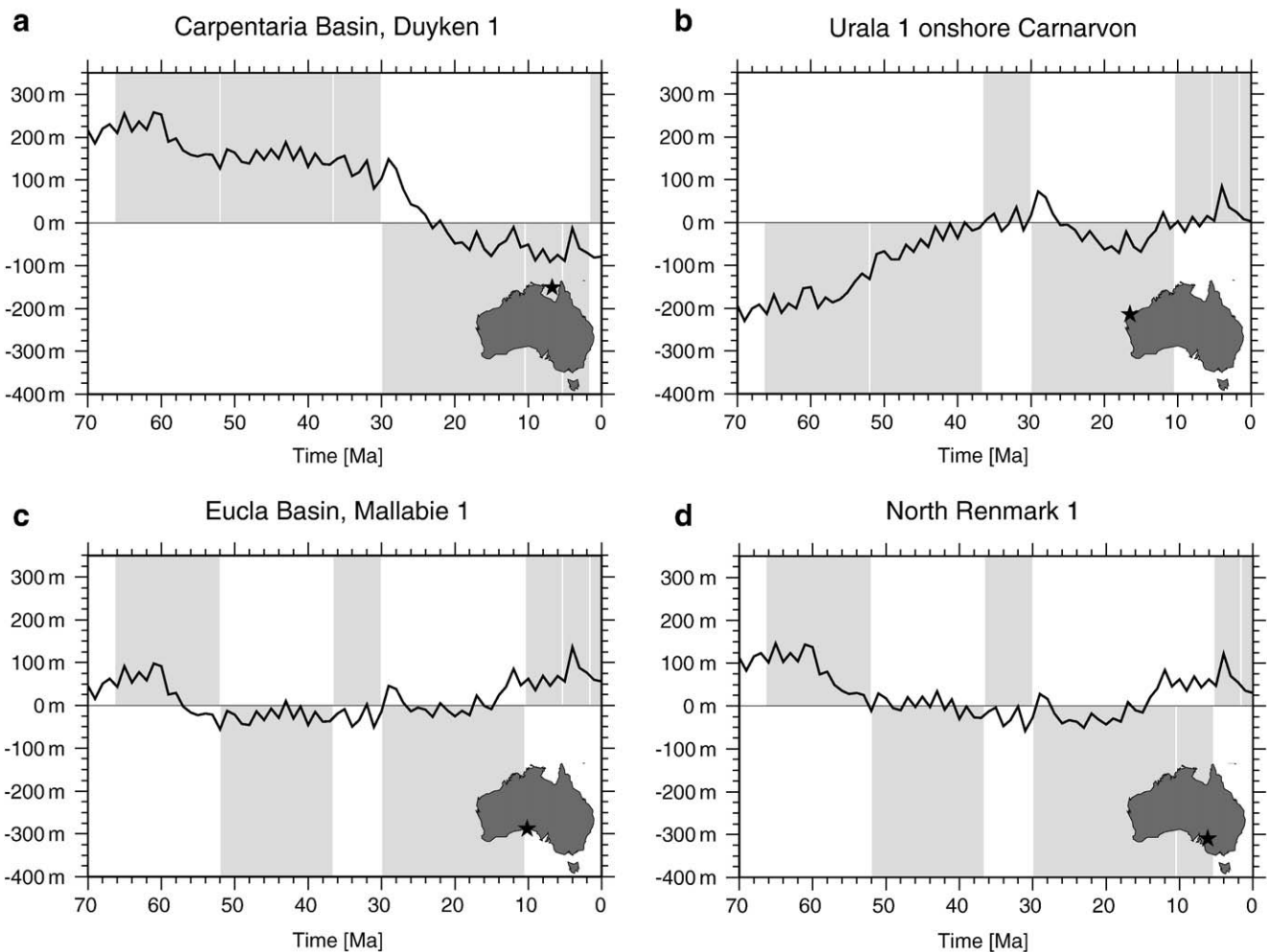


Fig. 6. Elevation history relative to sea level of 4 wells in Australia using an integrated model which combines dynamic topography, plate kinematics, eustatic sea level (Haq and Al-Qahtani, 2005) and sediment correction derived from Langford et al. (1995) and other sources. Gray rectangles in background indicate paleo-environment based on Langford et al. (1995) where a rectangle below 0 m elevation indicates flooding, and above 0 m indicates exposure above sea level for the respective location at given time. If the modelled curve is located within a gray rectangle, the observations are qualitatively matched. Dynamic topography model is scaled empirically by a factor of 0.55.

200 ± 50 m is seen between 36 and 30 Ma. The short-wavelength of this pulse precludes it being caused entirely by mantle-driven dynamic topography, however, another pulse of accelerated subsidence occurs in the last 10 million years. The water depth errors (Fig. 5d) would allow these two pulses to be less extreme, with continued accelerated subsidence occurring in the period between 30 and 10 Ma. Our dynamic topography model (Fig. 5d) predicts roughly the observed magnitude of tectonic subsidence both between 66 and 38 Ma, as well as after 10 Ma, providing convincing evidence that most observed Tertiary tectonic subsidence of the area, with the exception of the rapid subsidence pulse from 36 to 30 Ma, is indeed mantle convection driven.

6. Summary and discussion

The Australian Cenozoic surface topography has been significantly altered by transient, mantle convection-induced surface displacement and eustatic sea level changes. Using our integrated method, we can model spatial and temporal changes in the paleogeography of Australia which are well in agreement with the observed geological record. Matching of paleogeographic data with a dynamic topography model based on the S2ORTS seismic tomographic model (Ritsema et al., 1999) and the sea level estimate by Haq and Al-Qahtani (2005), the maximum amplitudes of dynamic topography affecting the Australian region during the Cenozoic can be estimated to be in the order of 500–600 m.

The Australian continent has been situated in the interior of the Indo-Australian plate during most of the Cenozoic. Localised and regional tectonic processes such as a changing Cenozoic intraplate stress regime (Dyksterhuis and Müller, 2008; Dyksterhuis et al., 2005; Célerier et al., 2005; Sandiford et al., 2004; Coblenz et al., 1995), rifting and wrench tectonics (along the southern Australian margin in the Cretaceous/Earliest Tertiary; Norvick and Smith, 2001), flexure (Haddad and Watts, 1999 in northern Australia; Quigley et al., 2007 in South Australia) and volcanism (Pliocene–Pleistocene, southeast Australia; Demidjuk et al., 2007; Roy et al., 2000) are other likely causes for surface deflection. However, these processes usually affect smaller areas and yield different geometrical patterns (e.g. narrow, elongated depressions due to foreland loading) compared to the continent-scale inundation patterns we focus on in this study. Low-amplitude, localised surface deflections do not have a significant impact on the continental inundation patterns.

The falling global eustatic sea level in the Cenozoic is largely counterbalanced and partly outpaced by the effect of an increasing negative dynamic topography in the Australian region, due to the motion of Australia toward the long-term Tethyan/Pacific slab burial ground in Southeast Asia. This significantly affects the flooding history of large epicontinental basins such as the Gulf of Carpentaria, the Murray–Darling basin and the Eucla basin.

Fig. 6 shows the modelled elevation for four wells, comparing our predicted elevation with the paleo-environment indicators (submerged, depositional vs. elevated, erosional) as reported by Langford et al. (1995). Our models successfully predict the Cenozoic paleo-elevation history for all four locations qualitatively. Data from the North Renmark 1 (Fig. 6d) and Mallalie 1 (Fig. 6c) locations in the Murray and Eucla Basin, respectively, indicates clearly shallow marine to low subaerial exposure for both locations, most likely not exceeding 60 m of water depths (Lukasik et al., 2000) in the Murray Basin, and marginal marine to fluvial environments with partly glauconitic facies for the eastern Eucla Basin (Hou et al., 2006). Lacking detailed stratigraphic data for the Duyken-1 (Fig. 6a) and Urala-1 (Fig. 6b) wells do not allow a rigorous quantitative assessment of our modelled paleo-elevations, however, reported unconformities and depositional cycles indicate a good fit.

The differences between our modelled topography and the observed paleogeography based on Langford et al. (1995) are expressed by calculating the area between modelled and observed paleo-shorelines through time and deriving the amount of inundation relative to the present-day 200 m isobath (Fig. 7). A particularly good fit for the whole continent is achieved for ages > 60 Ma, 36–31 Ma, and 11–9 Ma. Between 60–36 Ma, our models differ by up to 7% from the computed inundation based on Langford et al. (1995). Similarly, the period between 30–11 Ma shows up to 20% difference between predicted and observed inundation. Responsible for these big discrepancies between model and observations is the fact, that the flooding of the vast Eucla basin, both during Eocene and Miocene is not reproducible with our models. We attribute this mismatch to processes in the lithosphere, which are not taken into account in our models. DiCaprio et al. (2009) also observed that short-wavelength signals, not predicted by mantle-convection models, are required in order to predict the flooding history of the Eucla Basin.

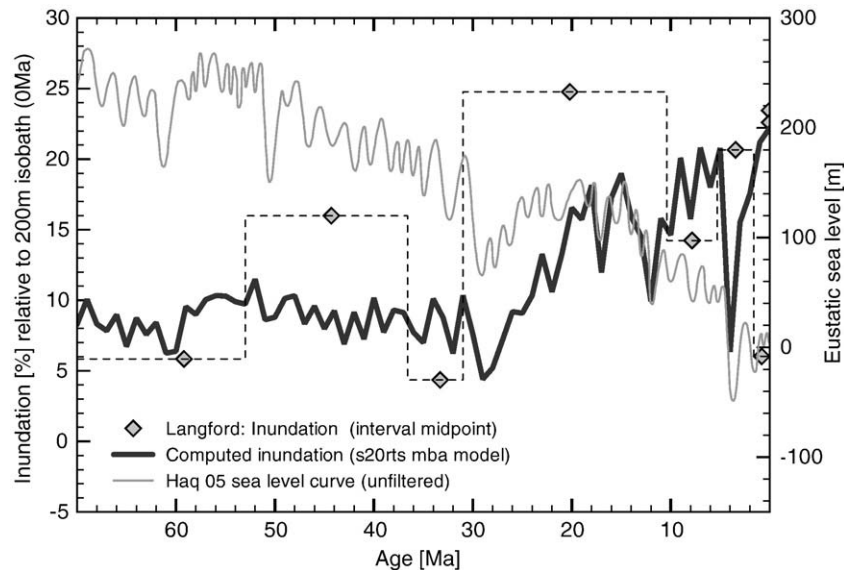


Fig. 7. Inundation of the Australian continental area over the past 70 Ma using our integrated paleo-topography model. Dynamic topography input is scaled by a factor of 0.55. Inundation is measured as % of the total continental area above the present-day 200 m isobath which is flooded at any given time. Diamonds and thin black dashed line shows the inundation estimate using the observations from Langford et al. (1995). Solid gray line shows the eustatic sea level used (Haq and Al-Qahtani, 2005).

7. Conclusions

The approach of integrating mantle convection-induced dynamic topography, eustatic sea level variations, plate kinematic and geologic data provides a powerful method to investigate the dynamic Earth system. It allows to qualitatively and quantitatively assess the dynamic paleogeography of stable continental platforms, the contribution of mantle-induced surface topography on observed regional anomalous epeirogenic processes and with it the changes occurring in the erosional domains, the sediment routing and depositional systems.

In particular, our model suggests that:

- From the Paleocene to the Eocene Australia gradually moved over a dynamic topography low which was centered around the Canning Basin area at the beginning of the Tertiary, driven by a slow northwestward absolute motion of Australia from about 65 to 45 Ma. This process resulted in a gradual uplift of the North West Shelf paired with subsidence of the Great Australian Bight area. The mantle downwelling is interpreted to reflect sinking slab material originally subducted along Australia's Cretaceous eastern Gondwana margin.
- Accelerated northward motion of Australia after 45 Ma shifted this dynamic topography low offshore to the Southern Ocean, contributing to a regression in the central Eucla Basin from the Late Eocene to the Mid-Oligocene, but the magnitude of the observed Eocene transgression and regression is not well captured in our model.
- From the Mid-Oligocene to the Mid-Miocene Australia's continued fast northward motion progressively placed the Gulf of Carpentaria and the Cape York Peninsula over the Melanesian slab burial ground, drawing down the entire northern half of the Australian continent, while southern Australia was placed over an east–west elongated band of less pronounced mantle downwelling. This resulted in moderate regional uplift, paired with a global sea level rise in the Early Miocene of similar magnitude.
- In post-Mid-Miocene times, the northern dynamic topography low progressively affected areas further south, reaching latitudes of about 30° S (in a reference frame keeping Australia fixed in current coordinates) as Australia progressively moved northwards over subducted slab material. However, the dynamic topography amplitudes along the southern coast did not change markedly over the last 15 Myrs according to our model, implying a north-down scenario rather than only a tilting of the entire Australian continent with its northern part going down and its southern part going up during this period.
- Combined with a falling global sea level, the relative lack of change in dynamic topography since the Mid-Miocene resulted in renewed exposure of the Eucla Basin, paired with a transgression in the Gulf of Carpentaria, where subsidence rates exceeded rates of long-term sea level fall.

We demonstrate that the northward motion of the Australian continent resulted in large lateral displacement relative to the underlying mantle which induced complex warping of the Australian surface topography over the past 70 Ma. Based on our modelling, we conclude that the mantle-induced surface topography for the Australian continent during the Cenozoic was not larger than 600 m in amplitude and in average similar to the amplitudes of eustatic sea level change.

We are not able to reproduce the overall transgression and regression patterns in the Eucla Basin along the Great Australian Bight. This indicates that shallow lithospheric heterogeneities might have played a more dominant role, which might have been related to the style of passive margin evolution and early spreading history in the Australia–Antarctica system.

Our results have implications not only for reconstructing the creation and destruction of sediment accommodation space, but also for understanding the effects of deep Earth dynamics on the evolution of sediment source- and routing systems and the depositional

architecture in large intracontinental basins. Lastly, these mantle-induced surface deflections might have a significant effect on the evolution of petroleum systems in hydrocarbon-bearing basins.

Acknowledgements

We acknowledge Mike Sandiford for valuable discussions on the Australian flooding history. Nicholas Rawlinson and Wouter Schellart are thanked for editorial assistance. An anonymous reviewer and Mark Quigley provided many constructive remarks and helped to significantly improve the manuscript. This work was partly funded by an ARC linkage grant with ExxonMobil Upstream Research. Figures for this publication have been generated using the Generic Mapping Tools (Wessel and Smith, 1998). The electronic supplementary information contains two QuickTime animations.

Appendix A. Supplementary data

Supplementary data associated with this article can be found, in the online version at doi:10.1016/j.tecto.2009.08.028.

References

- Allen, P.A., Allen, J.R., 2005. *Basin Analysis: Principles and Applications* 2nd Edition. Blackwell Publishing, Incorporated, Oxford OX4 1JF, United Kingdom.
- Artemieva, I.M., 2003. Lithospheric structure, composition, and thermal regime of the East European Craton: implications for the subsidence of the Russian Platform. *Earth Planet. Sci. Lett.* 213, 431–446. doi:10.1016/S0012-821X(03)00327-3.
- Berggren, W.A., Kent, D.V., Swisher III, C.C., Aubry, M.P., 1995. A Revised Cenozoic Geochronology and Chronostratigraphy. In: Berggren, W.A., et al. (Ed.), *Geochronology, Time Scales, and Global Stratigraphic Correlation*. Vol. 54 of Special Publication: SEPM Soc. Sediment. Geol., pp. 129–212.
- Bond, G.C., 1978. Speculations on real sea-level changes and vertical motions of continents at selected times in the Cretaceous and Tertiary periods. *Geology* 6, 247–250.
- Brown, B., Müller, R.D., Struckmeyer, H.I.M., 2001. Anomalous tectonic subsidence of the Southern Australian passive margin: response to cretaceous dynamic topography or differential lithospheric stretching. PESA Eastern Australian Basins Symposium, Melbourne, Vic. 5, pp. 563–570. 25–28 Nov.
- Burgess, P.M., Gurnis, M., 1995. Mechanisms for the formation of cratonic stratigraphic sequences. *Earth Planet. Sci. Lett.* 136, 647–663.
- Célerier, J., Sandiford, M., Hansen, D.L., Quigley, M., 2005. Modes of active intraplate deformation, Flinders Ranges, Australia. *Tectonics* 24, TC6006. doi:10.1029/2004TC001679.
- Christie-Blick, N., Driscoll, N.W., 1995. Sequence stratigraphy. *Ann. Rev. Earth Planet. Sci.* 23 (1), 451–478. doi:10.1146/annurev.ea.23.050195.002315.
- Clarke, J.D.A., Gammon, P.R., Hou, B., Gallagher, S.J., 2003. Middle to Upper Eocene stratigraphic nomenclature and deposition in the Eucla Basin. *Aust. J. Earth Sci.* 50 (2), 231–248. doi:10.1046/j.1440-0952.2003.00995.x.
- Cluzel, D., Aitchison, J.C., Picard, C., 2001. Tectonic accretion and underplating of mafic terranes in the Late Eocene intraoceanic fore-arc of New Caledonia (Southwest Pacific): geodynamic implications. *Tectonophysics* 340 (1–2), 23–59. doi:10.1016/S0040-1951(01)00148-2.
- Coblentz, D.D., Sandiford, M., Richardson, R.M., Zhou, S., Hillis, R.R., 1995. The origins of the intraplate stress field in continental Australia. *Earth Planet. Sci. Lett.* 133, 299–309.
- Conrad, C.P., Gurnis, M., 2003. Seismic tomography, surface uplift, and the breakup of Gondwanaland: integrating mantle convection backwards in time. *Geochem. Geophys. Geosyst.* 4 (3), 1031. doi:10.1029/2001GC000299.
- Conrad, C.P., Lithgow-Bertelloni, C., Loudon, K.E., 2004. Iceland, the Farallon slab, and dynamic topography of the North Atlantic. *Geology* 32 (3), 177–180. doi:10.1130/G20137.1.
- de Broekert, P., Sandiford, M., 2005. Buried inset-valleys in the Eastern Yilgarn Craton, Western Australia: geomorphology, age, and allogenic control. *J. Geol.* 113 (4), 471–493.
- Demidjuk, Z., Turner, S., Sandiford, M., George, R., Foden, J., Etheridge, M., 2007. U-series isotope and geodynamic constraints on mantle melting processes beneath the Newer Volcanic Province in South Australia. *Earth Planet. Sci. Lett.* 261 (3–4), 517–533. doi:10.1016/j.epsl.2007.07.006.
- DiCaprio, L., Gurnis, M., Müller, R.D., 2009. Long-wavelength tilting of the Australian continent since the Late Cretaceous. *Earth Planet. Sci. Lett.* 278, 175–185. doi:10.1016/j.epsl.2008.11.030.
- Duddy, I.R., 2003. Mesozoic: a time of change in tectonic regime. In: Birch, W.D. (Ed.), *Geology of Victoria*. Special Publication, 23. Geological Society of Australia, Victoria Division, pp. 239–286. Ch. 9.
- Dyksterhuis, S., Müller, R.D., 2008. Cause and evolution of intraplate orogeny in Australia. *Geology* 36 (6), 495–498. doi:10.1130/G24536A.1.
- Dyksterhuis, S., Müller, R.D., Albert, R.A., 2005. Paleostress field evolution of the Australian continent since the Eocene. *J. Geophys. Res.* 110 (B5), B05102. doi:10.1029/2003JB002728.
- Exon, N.F., Colwell, J.B., 1994. Geological history of the outer North West Shelf of Australia: a synthesis. *AGSO Journal of Australian Geology & Geophysics* 15 (1), 177–190.

- Finn, C.A., Müller, R.D., Panter, K.S., 2005. A Cenozoic diffuse alkaline magmatic province (DAMP) in the southwest Pacific without rift or plume origin. *Geochem. Geophys. Geosyst.* 6 (2), Q02005. doi:10.1029/2004GC000273.
- Fishwick, S., Heintz, M., Kennett, B.L., Reading, A.M., Yoshizawa, K., 2008. Steps in lithospheric thickness within eastern Australia, evidence from surface wave tomography. *Tectonics* 27, TC4009. doi:10.1029/2007TC002116.
- Fishwick, S., Kennett, B.L., Reading, A.M., 2005. Contrasts in lithospheric structure within the Australian craton—insights from surface wave tomography. *Earth Planet. Sci. Lett.* 231, 163–176. doi:10.1016/j.epsl.2005.01.009.
- Gaina, C., Müller, R.D., 2007. Cenozoic tectonic and depth/age evolution of the Indonesian gateway and associated back-arc basins. *Earth-Sci. Rev.* 83, 177–203. doi:10.1016/j.earscirev.2007.04.004.
- Gaina, C., Müller, R.D., Royer, J.-Y., Stock, J., Hardebeck, J., Symonds, P., 1998. The tectonic history of the Tasman Sea: a puzzle with 13 pieces. *J. Geophys. Res.* 103 (B6), 12413–12433.
- Gallagher, S.J., Gourley, T.L., 2007. Revised Oligo-Miocene stratigraphy of the Murray Basin, southeast Australia. *Aust. J. Earth Sci.* 54, 837–849. doi:10.1080/08120090701392705.
- Gradstein, F., Ogg, J., Smith, A., Agterberg, F., Bleeker, W., Cooper, R., Davydov, V., Gibbard, P., Hinnov, L., House, M., Lourens, L., Luterbacher, H., McArthur, J., Melchin, M., Robb, L., Shergold, J., Villeneuve, M., Wardlaw, B., Ali, J., Brinkhuis, H., Hilgen, F., Hooker, J., Howarth, R., Knoll, A., Laskar, J., Monechi, S., Plumb, K., Powell, J., Raffi, I., Röhl, U., Sadler, P., Sanfilippo, A., Schmitz, B., Shackleton, N., Shields, G., Strauss, H., Van Dam, J., van Kolfschoten, T., Veizer, J., Wilson, D., 2004. *A Geologic Time Scale*. Cambridge University Press. URL <http://www.stratigraphy.org>.
- Grand, S.P., van der Hilst, R.D., Widiyantoro, S., 1997. Global seismic tomography; a snapshot of convection in the Earth. *GSA Today* 7 (4), 1–7.
- Gurnis, M., 1990. Bounds on global dynamic topography from Phanerozoic flooding of continental platforms. *Nature* 344, 754–756.
- Gurnis, M., 2001. Sculpting the Earth from inside out. *Sci. Amer.* 284, 40–48.
- Gurnis, M., Müller, R.D., Moresi, L.N., 1998. Cretaceous vertical motion of Australia and the Australian–Antarctic discordance. *Science* 279, 1499–1504.
- Haddad, D., Watts, A.B., 1999. Subsidence history, gravity anomalies, and flexure of the northeast Australian margin in Papua New Guinea. *Tectonics* 18 (5), 827–842. doi:10.1029/1999TC900009.
- Hager, B.H., O'Connell, R.J., 1981. A simple global model of plate dynamics and mantle convection. *J. Geophys. Res.* 86, 4843–4867.
- Hall, R., 1998. The Plate Tectonics of Cenozoic SE Asia and the Distribution of Land and Sea. In: Hall, R., Holloway, J.D. (Eds.), *Biogeography and Geological evolution of SE Asia*. Blackhuys Publisher, Leiden, pp. 99–131.
- Hall, R., 2002. Cenozoic geological and plate tectonic evolution of SE Asia and the SW Pacific: computer-based reconstructions, model and animations. *J. Asian Earth Sci.* 20 (4), 354–431.
- Hall, R., Wilson, M.E.J., 2000. Neogene sutures in eastern Indonesia. *J. Asian Earth Sci.* 18, 781–808.
- Hallam, A., 1984. Pre-Quaternary sea-level changes. *Ann. Rev. Earth Planet. Sci.* 12, 205–243.
- Haq, B.U., Al-Qahtani, A.M., 2005. Phanerozoic cycles of sea-level change on the Arabian Platform. *GeoArabia* 10 (2), 127–160.
- Haq, B.U., Hardenbol, J., Vail, P.R., 1987. Chronology of fluctuating sea levels since the Triassic. *Science* 235, 1156–1167.
- Harrowfield, M.J., Keep, M., 2005. Tectonic modification of the Australian North-West Shelf: episodic rejuvenation of long-lived basin divisions. *Basin Research* 17, 225–239. doi:10.1111/j.1365-2117.2005.00251.x.
- Hinschberger, F., Malod, J.-A., Réhault, J.-P., Villeneuve, M., Royer, J.-Y., Burhanuddin, S., 2005. Late Cenozoic geodynamic evolution of eastern Indonesia. *Tectonophysics* 404, 91–118. doi:10.1016/j.tecto.2005.05.005.
- Hou, B., Alley, N.F., Frakes, L.A., Stoian, L., Cowley, W.M., 2006. Eocene stratigraphic succession in the Eucla Basin of South Australia and correlation to major regional sea-level events. *Sed. Geol.* 183, 297–319. doi:10.1016/j.sedgeo.2005.10.007.
- Hou, B., Frakes, L.A., Sandiford, M., Worrall, L., Keeling, J., Alley, N.F., 2008. Cenozoic Eucla Basin and associated palaeovalleys, southern Australia — climatic and tectonic influences on landscape evolution, sedimentation and heavy mineral accumulation. *Sedimentary Geology* 203 (1–2), 112–130. doi:10.1016/j.sedgeo.2007.11.005.
- Jordan, T.H., 1978. Composition and development of the continental tectosphere. *Nature* 274, 544–548. doi:10.1038/2745444a0.
- Jordan, T.H., 1988. Structure and formation of the continental tectosphere. *J. Petrology Special Lithosphere Issue* 11–37.
- Kamp, P.J.J., 1986. The mid-Cenozoic Challenger Rift System of western New Zealand and its implications for the age of Alpine fault inception. *Geol. Soc. Am. Bull.* 97 (3), 255–281. doi:10.1130/0016-7606(1986)97<255:TMCRSO>2.0.CO;2.
- Karato, S., 1993. Importance of anelasticity in the interpretation of seismic tomography. *Geophys. Res. Lett.* 20, 1623–1626.
- Paleogeographic atlas of Australia. In: Langford, R., Wilford, G., Truswell, E.M., Isern, A.R. (Eds.), Volume 10 — Cainozoic. Australian Geological Survey Organization, Canberra.
- Lithgow-Bertelloni, C., Gurnis, M., 1997. Cenozoic subsidence and uplift of continents from time-varying dynamic topography. *Geology* 25 (8), 735–738.
- Lithgow-Bertelloni, C., Silver, P.G., 1998. Dynamic topography, plate driving forces and the African superswell. *Nature* 395.
- Lukasik, J.J., James, N.P., 2003. Deepening-upward subtidal cycles Murray Basin, South Australia. *J. Sedim. Res.* 73 (5), 653–671.
- Lukasik, J.J., James, N.P., McGowan, B., Bone, Y., 2000. An epeiric ramp: low-energy, cool-water carbonate facies in a Tertiary inland sea, Murray Basin, South Australia. *Sedimentology* 47 (4), 851–881. doi:10.1046/j.1365-3091.2000.00328.x.
- McGowan, B., Holdgate, G.R., Li, Q., Gallagher, S.J., 2004. Cenozoic stratigraphic succession in southeastern Australia. *Aust. J. Earth Sci.* 51 (4), 459–496. doi:10.1111/j.1400-0952.2004.01078.x.
- Miall, A.D., 1992. Exxon global cycle chart: an event for every occasion? *Geology* 20, 787–790.
- Miller, K.G., Kominz, M.A., Browning, J.V., Wright, J.D., Mountain, G.S., Katz, M.E., Sugarman, P.J., Cramer, B.S., Christie-Blick, N., Pekar, S.F., 2005. The Phanerozoic record of global sea-level change. *Science* 310, 1293–1298. doi:10.1126/science.1116412.
- Mitrovica, J.X., Beaumont, C., Jarvis, G.T., 1989. Tilting of continental interiors by the dynamical effects of subduction. *Tectonics* 8 (5), 1079–1094.
- Müller, R.D., Gaina, C., Tikku, A., Mihut, D., Cande, S.C., Stock, J.M., 2000a. Mesozoic/Cenozoic tectonic events around Australia. The History and Dynamics of Global plate motions: of *Geophys. Monogr. Ser. AGU*, Vol. 121, pp. 161–188.
- Müller, R.D., Lim, V.S.L., Isern, A.R., 2000b. Late Tertiary tectonic subsidence on the northeast Australian passive margin: response to dynamic topography? *Mar. Geol.* 162, 337–352.
- Müller, R.D., Sdrolias, M., Gaina, C., Roest, W.R., 2008a. Age, spreading rates, and spreading asymmetry of the world's ocean crust. *Geochem. Geophys. Geosyst.* 9 (4), Q04006. doi:10.1029/2007GC001743.
- Müller, R.D., Sdrolias, M., Gaina, C., Steinberger, B., Heine, C., 2008b. Long-term sea-level fluctuations driven by ocean basin dynamics. *Science* 319 (5868), 1357–1362. doi:10.1126/science.1151540.
- Nielsen, S.B., Stephenson, R., Thomsen, E., 2007. Dynamics of Mid-Palaeocene North Atlantic rifting linked with European intra-plate deformations. *Nature* 450 (7172), 1071–1074. doi:10.1038/nature06379.
- Nielsen, S.B., Thomsen, E., Hansen, D.L., Clausen, O.R., 2005. Plate-wide stress relaxation explains European Palaeocene basins inversions. *Nature* 435, 195–198. doi:10.1038/nature03599.
- N.O.A.A., National Geophysical Data Center, 2006. ETOPO2v2 2-minute global relief. <http://www.ngdc.noaa.gov/mgg/fliers/06mgg01.html>.
- Norvick, M.S., Smith, M.A., 2001. Mapping the plate tectonic reconstruction of Southern and Southeastern Australia and implications for petroleum systems. *APPEA Journal* 49 (1), 15–35.
- O'Neill, C., Müller, R.D., Steinberger, B., 2003. Geodynamic implications of moving Indian Ocean hotspots. *Earth Planet. Sci. Lett.* 215, 151–168. doi:10.1016/S0012-821X(03)00368-6.
- Quigley, M.C., Sandiford, M., Cupper, M.L., 2007. Distinguishing tectonic from climatic controls on range-front sedimentation. *Basin Research* 19, 491–505. doi:10.1111/j.1365-2117.2007.00336.x.
- Ritsema, J., van Heijst, H.J., Woodhouse, J.H., 1999. Complex shear wave velocity structure imaged beneath Africa and Iceland. *Science* 286, 1925–1928. doi:10.1126/science.286.5446.1925.
- Roy, P.S., Whitehouse, J., Cowell, P.J., Oakes, G., 2000. Mineral sands occurrences in the Murray Basin, Southeastern Australia. *Economic Geology* 95, 1107–1128.
- Royer, J.-Y., Rollet, N., 1997. Plate-tectonic setting of the Tasmanian region. *Aust. J. Earth Sci.* 44 (5), 543–560. doi:10.1080/08120099708728336.
- Russell, M., Gurnis, M., 1994. The planform of epeirogeny: vertical motions of Australia during the Cretaceous. *Basin Research* 6, 63–76. doi:10.1111/j.1365-2117.1994.tb00076.x.
- Sahagian, D., Jones, M., 1993. Quantified Middle Jurassic to Paleocene eustatic variations based on Russian Platform stratigraphy: stage level resolution. *Geol. Soc. Am. Bull.* 105, 1109–1118.
- Sahagian, D., Pinous, O., Olfieriev, A., Zakharov, V., 1996. Eustatic curve for the Middle Jurassic–Cretaceous based on Russian platform and Siberian stratigraphy: zonal resolution. *AAPG Bulletin* 80 (9), 1433–1458.
- Sahagian, D., Watts, A.B., 1991. Introduction to the special section on measurement, causes and consequences of long-term sealevel change. *J. Geophys. Res.* 96, 6585–6589.
- Sandiford, M., 2003a. Geomorphic constraints on the Late Neogene tectonics of the Otway Range, Victoria. *Aust. J. Earth Sci.* 50 (1), 69–80. doi:10.1046/j.1440-0952.2003.00973.x.
- Sandiford, M., 2003b. Neotectonics of southeastern Australia: Linking the Quaternary faulting record with seismicity and in situ stress. In: Hillis, R. R., Müller, R. D. (Eds.), *Evolution and Dynamics of the Australian Plate*. Vol. 22 of *Geol. Soc. Aust. Spec. Publ.* 22 and *Spec. Paper Geol. Soc. Am.* 372. *Geol. Soc. of Australia and Geol. Soc. of America*, pp. 101–113.
- Sandiford, M., 2007. The tilting continent: a new constraint on the dynamic topographic field from Australia. *Earth Planet. Sci. Lett.* 261, 152–161. doi:10.1016/j.epsl.2007.06.023.
- Sandiford, M., Coblenz, D.D., Richardson, R.M., 1995. Ridge torques and continental collision in the Indian–Australian plate. *Geology* 23 (7), 653–656.
- Sandiford, M., Wallace, M.W., Coblenz, D.D., 2004. Origin of the in situ stress field in southeastern Australia. *Basin Res.* 16, 325–338. doi:10.1111/j.1365-2117.2004.00235.x.
- Sandwell, D.T., 2009. SRTM30_PLUS: SRTM30, Coastal & Ridge multibeam, estimated topography. ftp://topex.ucsd.edu/pub/srtm30_plus/.
- Schellart, W.P., 2007. North-eastward subduction followed by slab detachment to explain ophiolite obduction and Early Miocene volcanism in Northland, New Zealand. *Terra Nova* 19 (3), 211–218. doi:10.1111/j.1365-3121.2007.00736.x.
- Schellart, W.P., Lister, G.S., Toy, V.G., 2006. A Late Cretaceous and Cenozoic reconstruction of the Southwest Pacific region: tectonics controlled by subduction and slab rollback processes. *Earth-Science Rev.* 76, 191–233. doi:10.1016/j.earscirev.2006.01.002.
- Slater, J.G., Christie, P.A.F., 1980. Continental stretching: an explanation of the post-mid-Cretaceous subsidence of the Central North Sea Basin. *J. Geophys. Res.* 85 (B7), 3711–3739.
- Shapiro, S.S., Hager, B.H., Jordan, T.H., 1999. Stability and dynamics of the continental tectosphere. *Lithos* 48, 115–133.
- Simons, F.J., van der Hilst, R.D., 2002. Age-dependent seismic thickness and mechanical strength of the Australian lithosphere. *Geophys. Res. Lett.* 29 (11). doi:10.1029/2002GL014962.
- Simons, F.J., Zielhuis, A., van der Hilst, R.D., 1999. The deep structure of the Australian continent from surface wave tomography. *Lithos* 48, 17–43.

- Spasojević, S., Liu, L., Gurnis, M., Müller, R.D., 2008. The case for dynamic subsidence of the U.S. east coast since the Eocene. *Geophys. Res. Lett.* 35, L08305. doi:10.1029/2008GL033511.
- Stagg, H.M.J., Wilcox, J.B., Symonds, P.A., O'Brien, G.W., Colwell, J.B., Hill, P.J.A., Lee, C.-S., Moore, A.M.G., Struckmeyer, H.I.M., 1999. Architecture and evolution of the Australian continental margin. *AGSO Journal of Australian Geology & Geophysics* 17 (5/6), 17–33.
- Steckler, M.S., Watts, A.B., 1978. Subsidence of the Atlantic-type continental margin off New York. *Earth Planet. Sci. Lett.* 41 (1), 1–13.
- Steinberger, B., 2007. Effects of latent heat release at phase boundaries on flow in the Earth's mantle, phase boundary topography and dynamic topography at the Earth's surface. *Phys. Earth Planet. Int.* 164, 2–20. doi:10.1016/j.pepi.2007.04.021.
- Steinberger, B., Calderwood, A.R., 2006. Models of large-scale viscous flow in the Earth's mantle with constraints from mineral physics and surface observations. *Geophys. J. Int.* 167, 1461–1481. doi:10.1111/j.1365-246X.2006.03131.x.
- Steinberger, B., Schmeling, H., Marquart, G., 2001. Large-scale lithospheric stress field and topography induced by global mantle circulation. *Earth Planet. Sci. Lett.* 186, 75–91. doi:10.1016/S0012-821X(01)00229-1.
- Steinberger, B., Sutherland, R., O'Connell, R.J., 2004. Prediction of Emperor–Hawaii seamount locations from a revised model of global plate motion and mantle flow. *Nature* 430, 167–173. doi:10.1038/nature02660.
- Stoddard, P.R., Abbot, D., 1996. Influence of the tectosphere upon plate motions. *J. Geophys. Res.* 101 (B3), 5425–5433.
- Struckmeyer, H., Brown, P., 1990. Australian Sea Level Curves Part 1: Australian Inundation Curves, Palaeogeography. Tech. rep., Bureau of Mineral Resources, Geology and Geophysics Petroleum Division of the Australian Mineral Industries Research Association, GPO Box 378, Canberra, ACT 2601, Australia.
- Swain, C.J., Kirby, J.F., 2006. An effective elastic thickness map of Australia from wavelet transforms of gravity and topography using Forsyth's method. *Geophys. Res. Lett.* 33, L02314. doi:10.1029/2005GL025090.
- Trampert, J., Deschamps, F., Resovsky, J., Yuen, D.A., 2004. Probabilistic tomography maps chemical heterogeneities in the lower mantle. *Science* 306, 853–856. doi:10.1126/science.1101996.
- van der Hilst, R.D., Widiyantoro, S., Engdahl, E.R., 1997. Evidence of deep mantle circulation from global tomography. *Nature* 386, 578–584. doi:10.1038/386578a0.
- Veevers, J.J. (Ed.), 1984. *Phanerozoic Earth History of Australia*. No. 2 in Oxford Monographs on Geology and Geophysics. Clarendon Press, Oxford, United Kingdom.
- Veevers, J.J., 2001. Billion-year earth history of Australia and neighbours in Gondwanaland. GEMOC Press, Sydney, Australia.
- Veevers, J.J., Powell, C.M., Roots, S.R., 1991. Review of seafloor spreading around Australia. I. synthesis of the patterns of spreading. *Aust. J. Earth Sci.* 38 (4), 373–389.
- Watts, A.B., Thorne, J., 1984. Tectonics, global changes in sea level and their relationship to stratigraphical sequences at the US Atlantic continental margin. *Mar. Petrol. Geol.* 1, 3–19. doi:10.1016/0264-8172(84)90134-X.
- Wessel, P., Smith, W.H.F., 1998. New, improved version of Generic Mapping Tools released. *EOS Trans. Am. Geophys. Union* 79 (47), 579.
- West, B.P., Wilcock, W.S.D., Sempéré, J.-C., Géli, L., 1997. Three-dimensional structure of asthenospheric flow beneath the Southeast Indian Ridge. *J. Geophys. Res.* 102 (B4), 7783–7802. doi:10.1029/96JB03895.
- Wheeler, P., White, N., 2000. Quest for dynamic topography: observations from Southeast Asia. *Geology* 28 (11), 963–966.
- Whittaker, J.M., Müller, R.D., Leitchenkov, G., Stagg, H.M.J., Sdrölias, M., Gaina, C., Goncharov, A., 2007. Major Australian–Antarctic Plate reorganization at Hawaiian–Emperor bend time. *Science* 318, 83–86. doi:10.1126/science.1143769.
- Xie, X., Müller, R.D., Lia, S., Gong, Z., Steinberger, B., 2006. Origin of anomalous subsidence along the Northern South China Sea margin and its relationship to dynamic topography. *Mar. Petrol. Geol.* 23, 745–765. doi:10.1016/j.marpetgeo.2006.03.004.